Anal. Chem. **2004,** *76,* 823−832

Integration of Knowledge-Based Metabolic Predictions with Liquid Chromatography Data-Dependent Tandem Mass Spectrometry for Drug Metabolism Studies: Application to Studies on the Biotransformation of Indinavir

M. Reza Anari,* Rosa I. Sanchez, Ray Bakhtiar, Ronald B. Franklin, and Thomas A. Baillie

Department of Drug Metabolism, Merck Research Laboratories, WP75A-203, Sumneytown Pike, West Point, Pennsylvania 19486

Despite recent advances in the application of data-dependent liquid chromatography/tandem mass spectrometry (LC/MS/MS) to the identification of drug metabolites in complex biological matrixes, a prior knowledge of the likely routes of biotransformation of the therapeutic agent of interest greatly facilitates the detection and structural characterization of its metabolites. Thus, prediction of the $[M + H]^+$ m/z values of expected metabolites allows for the construction of user-defined MS^n protocols that frequently reveal the presence of minor drug metabolites, even in the presence of a vast excess of coeluting endogenous constituents. However, this approach suffers from inherent user bias, as a result of which additional "survey scans" (e.g., precursor ion and constant neutral loss scans) are required to ensure detection of as many drug-related components in the sample as possible. In the present study, a novel approach to this problem has been evaluated, in which knowledge-based predictions of metabolic pathways are first derived from a commercial database, the output from which is used to formulate a list-dependent LC/MS^n data acquisition protocol. Using indinavir as a model drug, a substructure similarity search on the MDL metabolism database with a similarity index of 60% yielded 188 "hits", pointing to the possible operation of two hydrolytic, two N-dealkylation, three N-glucuronidation, one N-methylation, and several aromatic and aliphatic oxidation pathways. Integration of this information with data-dependent LC/MS^n analysis using an ion trap mass spectrometer led to the identification of 18 metabolites of indinavir following incubation of the drug with human hepatic postmitochondrial preparations. This result was accomplished with only a single LC/MS^n run, representing significant savings in instrument use and operator time, and afforded an accurate view of the complex in vitro metabolic profile of this drug.

The biotransformation of drugs and other lipophilic xenobiotics commonly leads to the generation of a large number of metabolites, which may contribute to the efficacy and occasionally to the toxicity of the parent compound.[1] In many cases, metabolism is the primary mechanism of drug clearance from the body, and therefore, knowledge of the routes of metabolism in animals and humans and of the biological properties of the major biotransformation products represents an important objective in the development of new therapeutic agents.[2] In addition, an early assessment of metabolic pathways provides valuable information in the context of drug discovery efforts in that metabolic "soft spots" leading to rapid clearance or to the formation of reactive intermediates carrying a potential for toxicity can be recognized promptly and addressed by means of appropriate structural modifications.[3] Moreover, qualitative similarity between in vitro metabolic "profiles," typically obtained from incubations with liver preparations from animal species versus humans, serves to validate the selection of the nonrodent species for preclinical safety testing.[4] For these reasons, the development of improved analytical methodology for the rapid and sensitive detection and identification of drug metabolites in complex biological matrixes has assumed increasing importance in contemporary pharmaceutical research, which has become heavily reliant upon LC/MS and tandem MS-based analytical protocols.[5]

Despite recent advances in ionization methods, mass analyzers, and data acquisition and processing techniques, the ability to rapidly acquire multiple data sets on individual metabolites in a given sample to maximize structural information remains limited. Thus, while it has become possible to conduct multiple MS/MS experiments within a single LC run, affording product ion spectra of anticipated metabolites, separate LC analyses usually are required to obtain full scan, precursor ion scan, and constant neutral loss scan data in the search for metabolites whose structures may not have been anticipated.[5] Taking into account

* To whom correspondence should be addressed. Telephone: 215-652-0020. Fax: 215-652-2410. E-mail: reza_anari@merck.com.

(1) Guengerich, F. P. *Chem. Res. Toxicol.* **2001**, *14*, 611−650.
(2) Baillie, T. A.; Kassahun, K. *Adv. Exp. Med. Biol.* **2001**, *500*, 45−51.
(3) Watt, A. P.; Mortishire-Smith, R. J.; Gerhard, U.; Thomas, S. R. *Curr. Opin. Drug Discov. Devel.* **2003**, *6*, 57−65.
(4) Baillie, T. A.; Cayen, M. N.; Fouda, H.; Gerson, R. J.; Green, J. D.; Grossman, S. J.; Klunk, L. J.; LeBlanc, B.; Perkins, D. G.; Shipley, L. A. *Toxicol. Appl. Pharmacol.* **2002**, *182*, 188−196.
(5) Clarke, N. J.; Rindgen, D.; Korfmacher, W. A.; Cox, K. A. *Anal. Chem.* **2001**, *73*, 430A−439A.

10.1021/ac034980s CCC: $27.50
Published on Web 12/19/2003

the slow scan speed of commonly used triple quadrupole instruments compared to the time-of-flight mass analyzers,[6] this approach suffers from the need for iterative evaluation of a few metabolites at a time, which requires a relatively large amount of sample and a significant degree of user intervention. Intelligent data-dependent scripts have been developed in an attempt to address this problem and maximize the qualitative mass spectral information that may be obtained per analysis using triple quadrupole instruments.[7−9] More recently, the incorporation of data-dependent functionalities in MS software for ion traps, orthogonal Q-TOF, and linear ion trap instruments has allowed automatic switching of acquisition modes based upon user-defined criteria, resulting in a concomitant increase in the information content of the resulting mass spectral data.[10−14] Nevertheless, it has been our experience that a directed search for metabolites that are predicted on the basis of the structure of the parent compound offers the greatest probability of success in detecting drug-related materials in the presence of a relatively large excess of extraneous background. Such predictions, in turn, require knowledge of common biotransformation reactions exhibited by the functional groups present in the original drug molecule.

The goal of the present study was to explore a novel approach to drug metabolite analysis that integrates knowledge-based predictions of metabolic pathways (extracted from a commercial database) with LC/data-dependent tandem mass spectrometry. Indinavir (IND), an HIV-1 protease inhibitor known to undergo extensive metabolism both in vitro and in vivo, was selected as a model compound for the study, in which it was demonstrated that this integrated approach revealed essentially all major metabolites previously reported for this drug in human liver microsomal preparations from a single LC/MS^n analysis.

EXPERIMENTAL SECTION

Chemicals. Indinavir (Crixivan, MK-0639, L-735,524) [*N*-(2(*R*)-hydroxy-1(*S*)-indanyl)-2(*R*)-phenylmethyl-4(*S*)-hydroxy-5-(1-(4-(3-pyridylmethyl)-2(*S*)-*N*9-(*tert*-butylcarboxamido)piperazinyl)) pentanamide] was synthesized at the Merck Research Laboratories (West Point, PA). NADPH, uridine diphosphate glucuronic acid, dibasic sodium phosphate dihydrate, dibasic potassium phosphate, and magnesium chloride hexahydrate were purchased from Sigma Aldrich Inc. (St. Louis, MO). HPLC-grade acetonitrile was obtained from J. T. Baker (Phillipsburg, PA). Formic acid was purchased from GFS Chemicals (Columbus, OH), and HPLC-grade water was obtained from Mallinckrodt Baker, Inc. (Paris, KY). Pooled human hepatic postmitochondrial preparations (S9) were purchased from Gentest (Woburn, MA).

Safety Considerations. Human hepatic postmitochondrial preparations pose a safety risk from potential pathogenic contamination. Every batch of samples was handled by wearing appropriate protective clothing, restriction of work area access, and disinfection of exposed surfaces.

Indinavir Incubation with Human Hepatic Postmitochondrial Preparations. Incubations contained 1 mg/mL human hepatic S9 protein, 10 mM $MgCl_2$, 100 mM potassium phosphate buffer (pH 7.4), 2 mM uridine diphosphate glucuronic acid, and 10 μM IND. Samples were preincubated for 5 min at 37 °C in a shaking water bath. The reactions were initiated by addition of NADPH to a final concentration of 2 mM. The reaction was terminated after 1 h by removing 100 μL of the incubation mixture and mixing it with 0.2 mL of ice-cooled acetonitrile containing 0.1% formic acid. Samples were centrifuged at 3000 rpm for 10 min at 10 °C to pellet the denatured protein. The aqueous acetonitrile supernatants were concentrated under a gentle stream of nitrogen to 50% of its initial volume, and then transferred to the 96-well conical plates for the LC/MS^n analysis.

Knowledge-Based Metabolic Prediction for Indinavir Potential Metabolites. The MDL metabolite browser (version 2.3) was utilized to conduct the substructure similarity search on 8590 parent compounds and 53 373 transformations of the MDL Metabolite Database (MDL Information Systems, Inc.) in order to outline the potential metabolic pathways of IND. The MDL Metabolite Database contains published information on the biotransformations of drugs (1977−1983), pharmacokinetics (1986−1990), and original metabolism literature and new drug applications (1990−present). The substructural similarity search of 60% on the IND molecule resulted in 188 hits. All published biotransformations on the IND and its analogous were excluded to avoid bias in evaluation of the knowledge-based capability to predict the potential metabolic pathways of the IND. The substructure similarity search criteria that results in a reasonably wider range of hits (∼200) is preferred because this provides a better chance of predicting rare and unexpected reactions.

Calculation of Mass-to-Charge Ratios for Metabolites of Indinavir. The mass-to-charge ratios of all potential IND metabolites were calculated using an active spreadsheet that incorporates common biotransformation m/z changes of known enzymatic reactions. This biotransformation spreadsheet includes all classical primary metabolic pathways for xenobiotic biotransformations[15,16] as well as various multistage oxidative metabolic reactions encountered by the authors on various pharmaceuticals. These reactions that usually start with two-electron oxidation of the side chains often ends up with dealkylation or complete oxidation of alkyl sites to carboxylic acids, resulting in an unanticipated mass change of the parent drug (e.g., −42, −40, −28, −26, −14, −12, −0.0365, +2, +30, etc). The dealkylated products could also become the subject of further biotransformation reactions and, in the case of IND, both the protonated parent molecule and its expected major dealkylated metabolite were used as the starting masses. The less stringent similarity search retrieved many redundant reactions with similar mass-to-charge ratios. The

(6) Zhang, H.; Henion, J.; Yang, Y.; Spooner, N. *Anal. Chem.* **2000**, *72*, 3342−3348.
(7) Fernandez-Metzler, C. L.; Owens, K. G.; Baillie, T. A.; King, R. C. *Drug Metab. Dispos.* **1999**, *27*, 32−40.
(8) Yu, X.; Cui, D.; Davis, M. R. *J. Am. Soc. Mass Spectrom.* **1999**, *10*, 175−183.
(9) Gu, M.; Lim, H. K. *J. Mass Spectrom.* **2001**, *36*, 1053−1061.
(10) Lopez, L. L.; Yu, X.; Cui, D.; Davis, M. R. *Rapid Commun. Mass Spectrom.* **1998**, *12*, 1756−1760.
(11) Tiller, P. R.; Land, A. P.; Jardine, I.; Murphy, D. M.; Sozio, R.; Ayrton, A.; Schaefer, W. H. *J. Chromatogr., A* **1998**, *794*, 15−25.
(12) Lim, H. K.; Stellingweif, S.; Sisenwine, S.; Chan, K. W. *J. Chromatogr., A* **1999**, *831*, 227−241.
(13) Nassar, A. E.; Adams, P. E. *Curr. Drug Metab.* **2003**, *4*, 259−271.
(14) Xia, Y. Q.; Miller, J. D.; Bakhtiar, R.; Franklin, R. B.; Liu, D. Q. *Rapid Commun. Mass Spectrom.* **2003**, *17*, 1137−1145.
(15) Williams, R. T. *Detoxification Mechanisms: The metabolism and detoxication of drugs, toxic substances and other organic compounds*, 2nd ed.; John Willey & Sons, Inc.: New York, 1959.
(16) Testa, B.; Jenner, P. *Drug Metabolism: Clinical and Biological Aspects*, 1st ed.; Marcel Dekker: New York, 1976.

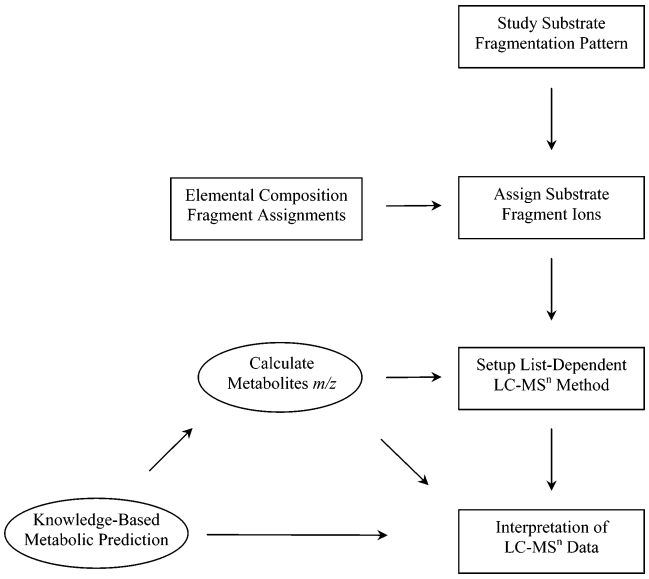

Figure 1. Metabolite identification strategy based on integration of knowledge-based metabolic predictions with liquid chromatography list-dependent tandem mass spectrometry.

calculated mass-to-charge ratios for all plausible metabolites of IND was exported to the Xcalibur LCQ software in order to set up a list-dependent instrument method.

Orthogonal Quadrupole Time-of-Flight Mass Spectrometry. The accurate mass measurements were carried out using a quadrupole orthogonal acceleration time-of-flight mass spectrometer (Q-ToF II, Micromass U.K. Ltd.), which was equipped with the LockSpray dual-electrospray ion source. The instrument was operated in the positive ion electrospray mode, and the experimental conditions were similar to those reported earlier.[17] The instrument was calibrated over a 150−700-Da mass range using a 0.1 ng/L solution of PEG 200/400/600 dissolved in acetonitrile/10 mM ammonium acetate (50:50 v/v). The ion m/z 283.1757, 371.2281, 432.2809, 503.3068, and 591.3592 from the PEG calibration solution were used as the reference peaks to provide exact mass measurement in the positive ESI mode. This solution was infused at ~5 μL/min through the reference spray via a Harvard 22 syringe pump (Harvard Apparatus Inc., South Natick, MA). For accurate mass studies of the protonated IND, a solution of IND (10 nM) in acidic mobile phase (aqueous 0.1% formic acid/methanol, 50:50 v/v) was infused at a flow rate adjusted to give an analyte spectrum of ~100 counts/s. Data were acquired in a continuum mode, and the accurate mass measurements and elemental compositions were carried out using the MassLynx software (version 3.4).

High Performance Liquid Chromatography Multistage Tandem Mass Spectrometry. The HPLC system used for analysis consisted of two pumps (LC10ADvp, Shimadzu Scientific Instruments Inc., Columbia, MD), a controller (SCL-10Avp), and a Perkin-Elmer series 200 autosampler (Norwalk, CT) with temperature control (10 °C). Separation of IND metabolites was accomplished on a Phenomenex Synergi 4μ Max-RP column (3 mm, 2 × 150 mm; Phenomenex, Torrance, CA). The mobile phase flowing through the column consisted of two eluants, solvent A (95% H_2O/5% acetonitrile, containing 0.1% formic acid, v/v) and solvent B (95% acetonitrile/5% H_2O, containing 0.1% formic acid, v/v). The column was maintained at initial conditions of 10% B for 3 min, followed by a linear gradient to 35% B over 50 min and then 90% B for 6 min. This condition was maintained for 4 min and then returned to the initial conditions over 3 min. The injection volume was 50 μL, and the flow rate was 0.3 mL/min, of which 0.075 mL/min was diverted into the mass spectrometer.

The LC/MS^n analysis was performed with a LCQ DECA XP ion-trap mass spectrometer (ThermoQuest, San Jose, CA) using an electrospray ion source. The mass spectrometer tune source parameters were optimized in the positive mode using a solution of IND as described above. The source voltage was maintained at 5 kV. Ions were sampled into the mass spectrometer at a maximum injection time of 300 ms. The first scan event was operated in full scan mode ranging from 100 to 900 Da. The second and third scan events were set as the list-dependent MS^n, using a relative collision energy of 30% with wideband activation features enabled. The isolation width was set to 2 Da, and ejected ions were detected with the electron multiplier set at a gain of 4 × 10^5. The product ion spectra of the metabolites in a list-dependent mode included the m/z 482, 483, 498, 523, 539, 555, 614, 630, 646, 659, 699,715, 790, and 806. Data acquisition and reduction were carried out using Xcalibur software (version 1.2).

Table 1. The Cycle of Scan Events for Indinavir Analysis Using LC/MS^n

scan no.	scan event
1	full scan MS [m/z 250−900]
2	data-dependent 177408n; [a]page/MS of most intense ion from parent list[b] in (1)
3	data-dependent scan; MS^{n}of second-most-intense ion from parent list in (2).

[a] The Wideband activation was enabled. [b] The list included m/z 482, 483, 498, 523, 539, 555, 614, 630, 646, 659, 699, 715, 790, and 806.

Table 2. Accurate Mass Measurements of the Major Ions Observed in the Electrospray CID Mass Spectrum of Protonated Indinavir

obs m/z	calcd m/z	error (ppm)	suggested elemental composition	assignment
614.3672	614.3706	−5.6	$C_{36}H_{48}N_5O_4$	$[M + H]^+$
596.3606	596.3601	0.9	$C_{36}H_{46}N_5O_3$	$-H_2O$
513.2895	513.2866	5.7	$C_{31}H_{37}N_4O_3$	$-(HCONHC_4H_9)$
495.2764	495.2760	0.8	$C_{31}H_{35}N_4O_2$	$-(HCONHC_4H_9 + H_2O)$
465.2874	465.2866	1.8	$C_{27}H_{37}N_4O_3$	$-C_9H_{11}ON$
421.2367	421.2365	0.4	$C_{25}H_{31}N_3O_3$	$-(HCONHC_4H_9 + C_6H_6N\cdot)$
364.2042	364.2025	4.6	$C_{22}H_{26}N_3O_2$	$-(HCONHC_4H_9 + C_9H_{11}ON)$
338.1755	338.1756	−0.3	$C_{21}H_{24}NO_3$	$-C_{15}H_{24}N_4O$
277.2005	277.2028	−8.3	$C_{15}H_{25}N_4O$	$-C_{21}H_{23}NO_3$

RESULTS AND DISCUSSION

The advent of new ion sources and mass analyzers, along with the recent advancement in data-acquisition and handling softwares, have significantly improved quality and detailed information acquired for identification of unknown structures. Despite recent advances in data-dependent qualitative mass spectrometry, the analysis of biological samples for metabolite identification purposes often requires prior knowledge of analytes' masses to successfully

(17) Anari, M. R.; Bakhtiar, R.; Franklin, R. B.; Pearson, P. G.; Baillie, T. A. *Anal. Chem.* **2003**, *75*, 469−478.

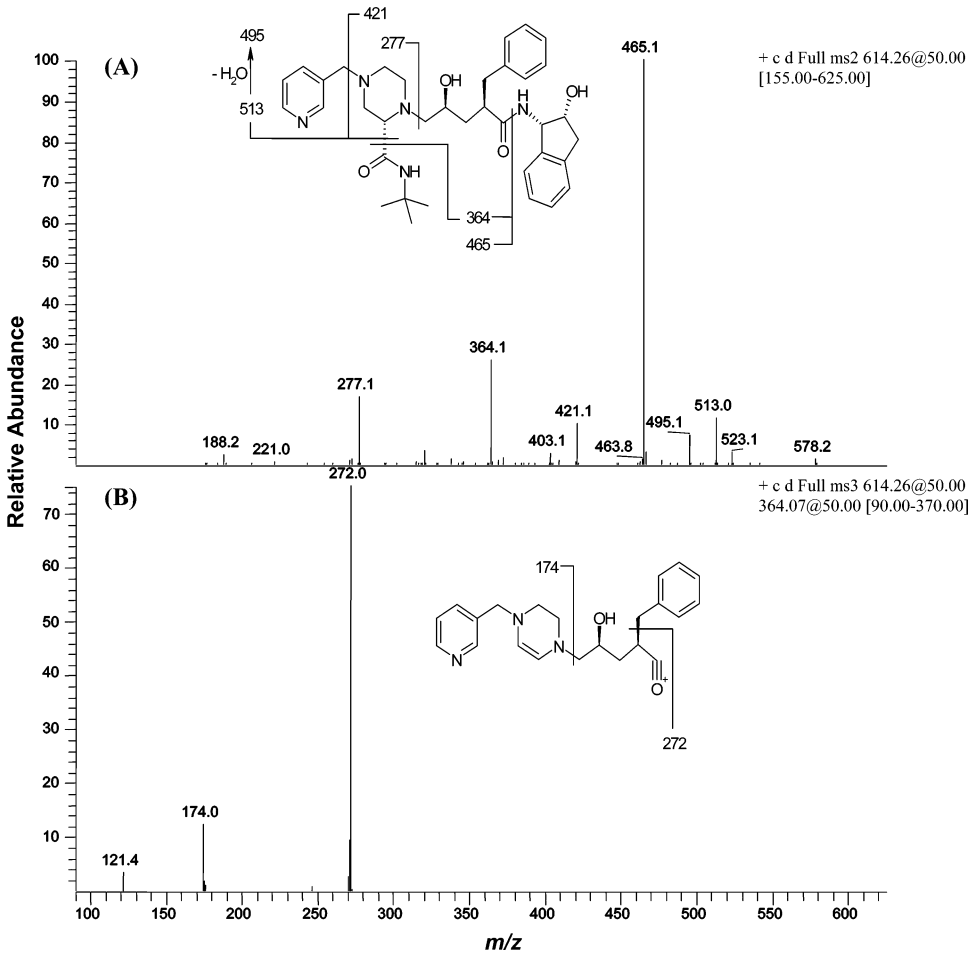

Figure 2. Product ion spectra of protonated indinavir; (A) MS^2 product ion spectrum of *m*/*z* 614 and (B) MS^3 product ion spectrum of *m*/*z* 364.

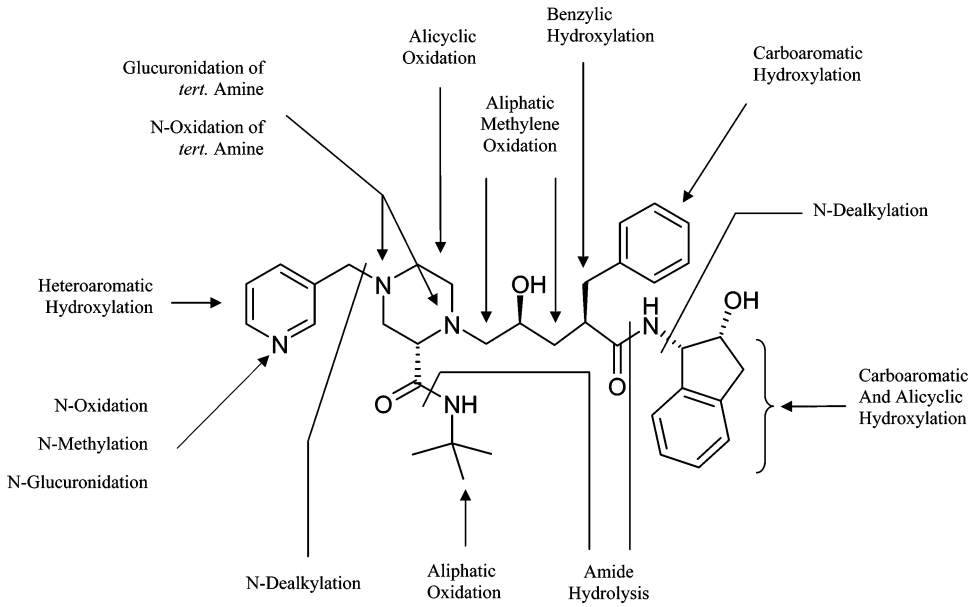

Figure 3. Knowledge-based metabolic prediction of indinavir.

acquire the metabolites' MS/MS or MS^n spectrum against the overwhelming and interfering signals from biological matrixes.[7,8,10] This, in turn, necessitates a prerequisite knowledge of metabolites' mass-to-charge ratios, which could be predicted on the basis of the knowledge of metabolism of functional groups present in the molecule.[15,16] The present study describes a new metabolite identification strategy, using indinavir as a model compound with well-characterized metabolic pathways,[18−20] which integrates prerequisite knowledge-based predictions with the liquid chroma-

(18) Chiba, M.; Hensleigh, M.; Nishime, J. A.; Balani, S. K.; Lin, J. H. *Drug Metab. Dispos.* **1996**, *24*, 307−314.

Table 3. Common Biotransformation *m/z* Changes Following Enzymatic Reactions

metabolic reaction	description	monoisotopic mass change	$[M+H]^+$ m/z[a]	
			substrate	dealkylated
substrate: $C_{36}H_{48}N_5O_4$	$[indinavir + H]^+$		614.4	523.3
$R-CH_2C_6H_5 \rightarrow R-H$	debenzylation	−90.0468	524.3	433.3
$R-^{80}Br \rightarrow R-H$	reductive debromination	−78.9105	535.5	444.4
$R-CF_3 \rightarrow R-H$	trifluoromethyl loss	−67.9984	546.4	455.3
$2R-^{35}Cl \rightarrow 2R-H$	2 × reductive dechlorination	−67.9222	546.4	455.4
$R-^{80}Br \rightarrow R-OH$	oxidative debromination	−61.9156	552.5	461.4
$R-C(CH_3)_3 \rightarrow R-H$	*tert*-butyl dealkylation	−56.0624	558.3	467.3
$R-ONO_2 \rightarrow R-OH$	hydrolysis of nitrate esters	−44.9851	569.4	478.3
$R-COOH \rightarrow R-H$	decarboxylation	−43.9898	570.4	479.3
$R-CH(CH_3)_2 \rightarrow R-H$	isopropyl dealkylation	−42.0468	572.3	481.3
$R-CH_2COCH_2CH_2CH_3 \rightarrow R-COOH$	propyl ketone to acid	−40.0675	574.3	483.3
$R-C(CH_3)_3 \rightarrow R-OH$	*tert*-butyl to alcohol	−40.0675	574.3	483.3
$2R-F \rightarrow 2R-H$	2 × reductive defluorination	−35.9811	578.4	487.3
$R-^{35}Cl \rightarrow R-H$	reductive dechlorination	−33.9611	580.4	489.4
$R-CH_2OH \rightarrow R-H$	hydroxymethylene loss	−30.0106	584.4	493.3
$R-NO_2 \rightarrow R-NH_2$	nitro reduction	−29.9742	584.4	493.4
$R-CH_2OCH_2CH_2CH_3 \rightarrow R-COOH$	propyl ether to acid	−28.0675	586.3	495.3
$R-C_2H_5 \rightarrow R-H$	deethylation	−28.0312	586.3	495.3
$R-CO-R' \rightarrow R-R'$	decarboxylation	−27.9949	586.4	495.3
$R-CH_2COCH_2CH_3 \rightarrow R-COOH$	ethyl ketone to acid	−26.0519	588.3	497.3
$R-CH(CH_3)_2 \rightarrow R-OH$	isopropyl to alcohol	−26.0519	588.3	497.3
$R-CH_2-CH_2OH \rightarrow R-CH=CH_2$	alcohols dehydration	−18.0105	596.4	505.3
$R-CH=N-OH \rightarrow R-CN$	dehydration of oximes	−18.0105	596.4	505.3
$R-F \rightarrow R-H$	reductive defluorination	−17.9906	596.4	505.3
$R-^{35}Cl \rightarrow R-OH$	oxidative dechlorination	−17.9662	596.4	505.4
$RR'S=O \rightarrow RR'S$	sulfoxide to thioether	−15.9949	598.4	507.3
$R-NHNHR'C=S \rightarrow R-NHNHR'C=O$	thioureas to ureas	−15.9772	598.4	507.4
$R-CH_2OCH_2CH_3 \rightarrow R-COOH$	ethyl ether to acid	−14.0519	600.3	509.3
$R-CH_3 \rightarrow R-H$	demethylation	−14.0157	600.4	509.3
$R-C(CH_3)_3 \rightarrow R-COOH$	*tert*-butyl to acid	−12.0726	602.3	511.3
$R-CH_2COCH_3 \rightarrow R-COOH$	methyl ketone to acid	−12.0363	602.3	511.3
$R-CH_2CH_3 \rightarrow R-OH$	ethyl to alcohol	−12.0363	602.3	511.3
$R-CH_2-CH_2-CH_2-CH_2-R' \rightarrow R-CH=CH-CH=CH-R'$	two sequential desaturation	−4.0314	610.3	519.3
hydroxylation + dehydration	hydroxylation and dehydration	−2.0157	612.4	521.3
$R-CH_2-OH \rightarrow R-CHO$, $R-CHOH-R' \rightarrow R-CO-R'$	first/second alcohols to aldehyde/ketone	−2.0157	612.4	521.3
$R-CH_2-CH_2-R' \rightarrow R-CH=CH-R'$	desaturation	−2.0157	612.4	521.3
$C_5H_7N \rightarrow C_5H_5N$	1,4-dihydropyridines to pyridines	−2.0157	612.4	521.3
$R-F \rightarrow R-OH$	oxidative defluorination	−1.9957	612.4	521.3
$R-CHNH_2-R' \rightarrow R-CO-R'$	oxidative deamination to ketone	−1.0316	613.3	522.3
demethylation and methylene to ketone	demethylation and methylene to ketone	−0.0365	614.3	523.3
$R-CH(OH)CH_3 \rightarrow R-COOH$	2-ethoxyl to acid	−0.0363	614.3	523.3
$R-CH_2-NH_2 \rightarrow R-CH_2-OH$	oxidative deamination to alcohol	0.9840	615.4	524.3
$R-CH(CH_3)_2 \rightarrow R-COOH$	isopropyl to acid	1.9430	616.3	525.3
$R-CH_3 \rightarrow R-OH$	demethylation and hydroxylation	1.9792	616.3	525.3
$R-CO-R' \rightarrow R-CHOH-R'$	ketone to alcohol	2.0157	616.4	525.3
$R-CH_2-R' \rightarrow R-(C=O)-R'$	methylene to ketone	13.9792	628.3	537.3
hydroxylation and desaturation	hydroxylation and desaturation	13.9792	628.3	537.3
$R-CH=CH-R' \rightarrow R-C(O)C-R'$	alkene to epoxide	13.9792	628.3	537.3
$R-X \rightarrow R-X-CH_3$	(O, N, S) methylation	14.0157	628.4	537.3
$R-CH_2CH_3 \rightarrow R-COOH$	ethyl to carboxylic acid	15.9586	630.3	539.3
$R-H \rightarrow R-OH$	hydroxylation	15.9949	630.4	539.3
$R-NH-R' \rightarrow R-NOH-R''$, $RR'R''N \rightarrow RR'R''NO$	second/third amine to hydroxylamine/*N*-oxide	15.9949	630.4	539.3
$R-S-R' \rightarrow R-SO-R'$, $R-SO-R' \rightarrow R-OSO-R'$	thioether to sulfoxide, sulfoxide to sulfone	15.9949	630.4	539.3
$R-CH-CH-R' \rightarrow R-CH(O)-CH-R'$	aromatic ring to arene oxide	15.9949	630.4	539.3
$R-CH_2CH_3 \rightarrow R-CH-(OH)_2$	demethylation and two hydroxylation	17.9741	632.3	541.3
$R-CH=CH-R \rightarrow R-CH_2-CHOH-R'$	hydration, hydrolysis (internal)	18.0106	632.4	541.3
$R-CN \rightarrow R-CONH_2$	hydrolysis of aromatic nitriles	18.0106	632.4	541.3
hydroxylation and ketone formation	hydroxylation and ketone formation	29.9741	644.3	553.3
$C_nH_m \rightarrow C_nH_{m-2}O_2$	quinone formation	29.9741	644.3	553.3
$R-CH_3 \rightarrow R-COOH$	demethylation to carboxylic acid	29.9742	644.3	553.3
$R-H \rightarrow R-OCH_3$	hydroxylation and methylation	30.0105	644.4	553.3
2 × hydroxylation	2 × hydroxylation	31.9898	646.4	555.3
$RR'S \rightarrow RR'SO_2$	thioether to sulfone	31.9898	646.4	555.3
$R-CH=CH-R \rightarrow R-CHOH-CHOH$	alkenes to dihydrodiol	34.0054	648.4	557.3
$R-NH_2 \rightarrow R-NHCOCH_3$	acetylation	42.0106	656.4	565.3
3 × hydroxylation	3 × hydroxylation	47.9847	662.4	571.3
$R-SH \rightarrow R-SO_3H$	aromatic thiols to sulfonic acids	47.9847	662.4	571.3
$R-COOH \rightarrow R-CONHCH_2COOH$	glycine conjugation	57.0215	671.4	580.4
$R-OH \rightarrow R-OSO_3H$	sulfate conjugation	79.9568	694.3	603.3
$R-H \rightarrow R-OSO_3H$	hydroxylation and sulfation	95.9517	710.3	619.3
$R-COOH \rightarrow R-CONH-CHCH_2SH-COOH$	cysteine conjugation	103.0092	717.4	626.3
$R-COOH \rightarrow R-CONH-CH_2CH_2SO_3H$	taurine conjugation	107.0041	721.4	630.3
$RR'-CH_2 \rightarrow RR'-CH-SCH_2CHNH_2-COOH$	*S*-cysteine conjugation	119.0041	733.4	642.3
$-CO + C_6H_8O_6$	decarboxylation and glucuronidation	148.0372	762.4	671.4
$RR'-CH_2 \rightarrow RR'-CH-SCH_2CHNCOCH_3-COOH$	*N*-acetylcysteine conjugation	161.0147	775.4	684.3
$R-OH \rightarrow R-O-C_6H_8O_6$	glucuronide conjugation	176.0321	790.4	699.4
$+2(SO_3)$	2 × sulfate conjugation	191.9035	806.3	715.2
$R-H \rightarrow R-O-C_6H_8O_6$	hydroxylation + glucuronide	192.0270	806.4	715.4
$+ C_{10}H_{15}N_3O_5S$	GSH conjugation	289.0732	903.4	812.4
$-2H + C_{10}H_{15}N_3O_6S$	desaturation + *S*-GSH conjugation	303.0525	917.4	826.4
$+ C_{10}H_{15}N_3O_6S$	*S*-GSH conjugation	305.0682	919.4	828.4
$+ O + C_{10}H_{15}N_3O_6S$	epoxidation + *S*-GSH conjugation	321.0631	935.4	844.4
$+2(C_6H_8O_6)$	2 × glucuronide conjugation	352.0642	966.4	875.4

[a] The *m*/*z* 482, 483, 498, 523, 539, 555, 614, 630, 646, 659, 699, 715, 790, and 806 were utilized to set up the list-dependent instrument method, as described in the Experimental Section.

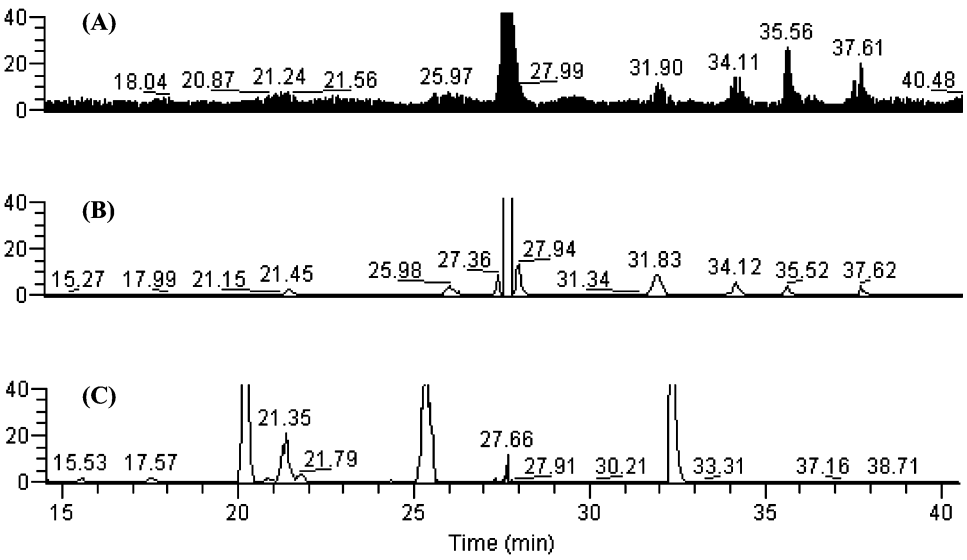

Figure 4. Total ion chromatogram (A), full data-dependent MS^2 ion chromatogram (B), and list-dependent MS^2 ion chromatogram for *m*/*z* 603 and 523 (C) from the incubation of indinavir with human hepatic postmitochondrial preparations.

tography data-dependent multistage tandem mass spectrometry (Figure 1).

On the basis of this approach, the knowledge-based metabolic prediction and metabolites' *m*/*z* calculations were carried on parallel to the study of substrate fragmentation pattern before setting up a list-dependent LC/MS^n instrument method (Figure 1). In addition, the interpretation of substrate tandem spectrum and assignment of the fragment structure was aided by the elemental composition data at the early stage.[5] This revealed the radical cation nature of one of the IND fragment ions and assured proper assignment of all other product ions. The list-dependent LC/MS^n instrument method that incorporated the list of metabolites' *m*/*z* with scan event orders compatible with fragmentation pattern was utilized to identify all potential metabolites of IND. A detailed description of each step and discussion of the knowledge-based predictions are described in the following sections.

Tandem Mass Spectrometry and Fragmentation Pattern of Indinavir. The product ion spectrum of IND under positive electrospray ionization obtained by LCQ-DECA (Figure 2) resulted in a major ion at *m*/*z* 465, as shown previously.[10] The high intensity of the *m*/*z* 465, formed by the neutral loss of 2-hydroxy-1-aminoindan moiety, could be explained by the inductive cleavage of the amide nitrogen atom as well as α cleavage of the amide carbonyl group.

However, using the new wideband activation feature that applies wider wave function fragmentation energy, we were able to see fragment ions at *m*/*z* 421, 364, and 277 directly in the MS^2 spectrum, similar to the MS/MS pattern of IND fragmentation obtained using triple quadruple instruments.[8,21] The second intense fragment ion, *m*/*z* 364, resulted from neutral loss of *tert*-butylformamide moiety from *m*/*z* 465 via α cleavage of the C−C bond adjacent to the carbonyl group. This ion was observed only in the MS^3 spectrum in an earlier multistage tandem mass spectrometry study when the wideband activation feature was not available.[10] Therefore, by characterizing the fragmentation pattern of IND, including the wideband activation feature, the MS^n data acquisition was set to fragment the second-most-intense ion detected in the MS^2 spectrum (Table 1), allowing skiping of one scan event that was generating the redundant product ions.[10] The

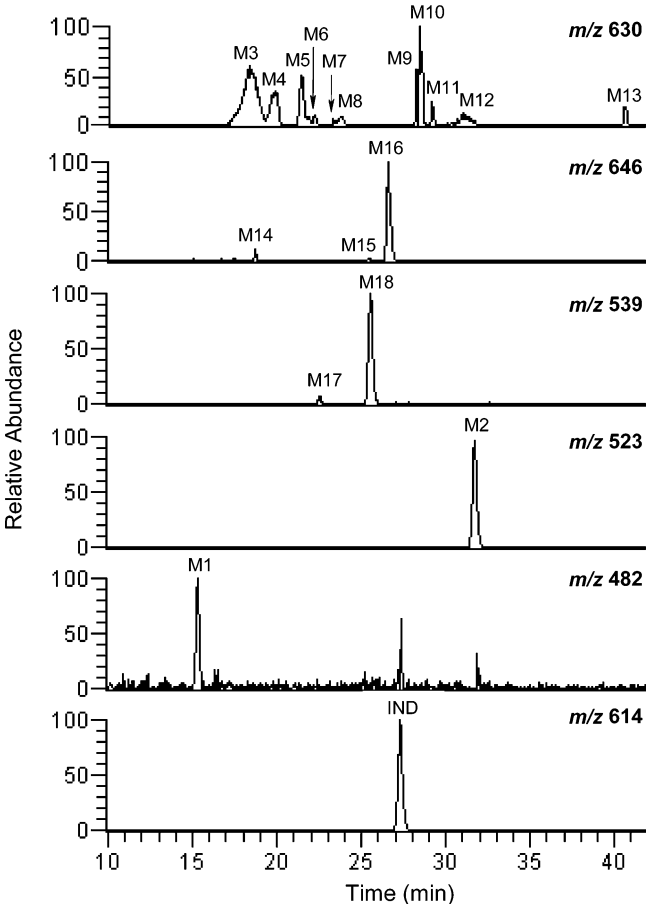

Figure 5. Reconstructed ion chromatograms of indinavir and its metabolites following incubation with human hepatic S9 preparations.

(19) Balani, S. K.; Woolf, E. J.; Hoagland, V. L.; Sturgill, M. G.; Deutsch, P. J.; Yeh, K. C.; Lin, J. H. *Drug Metab. Dispos.* **1996**, *24*, 1389−1394.
(20) Chiba, M.; Nishime, J. A.; Neway, W.; Lin, Y.; Lin, J. H. *Xenobiotica* **2000**, *30*, 117−129.

Table 4. List of the Human Hepatic Microsomal Metabolites of Indinavir and Their Corresponding Metabolic Change and Major Fragment Ions

metabolite label	proposed metabolites	t_r[a]	m/z	major fragment ions
M1	− indan-2-ol	15.2	482	277, 364, 381, 289, 176
M2	− 3-methylpyridine	31.9	523	374, 356, 487, 422, 404, 273, 338
M3	+ O	18.2	630	465, 612, 364, 277, 529, 473, 511, 594
M4	+ O	19.6	630	481, 612, 380, 529, 277, 437, 511, 594
M5	+ O	21.2	630	465, 481, 612, 364, 277, 529, 437, 380, 336, 354
M6	+ O	21.9	630	465, 364, 612, 529, 437, 277
M7	+ O	23.0	630	465, 364, 612, 529, 437, 277
M8	+ O	23.5	630	481, 463, 380, 612, 437, 529, 514, 277
M9	+ O	27.9	630	481, 612, 380, 293, 363, 465, 512, 511
M10	+ O	28.2	630	481, 612, 380, 293, 363, 465, 512, 511
M11	+ O	28.9	630	338, 481, 465, 421, 612, 513, 364, 277, 511
M12	+ O	30.7	630	465, 612, 481, 364, 277, 529, 437, 380
M13	+ O	40.3	630	481, 293, 380, 511, 372, 494, 594
M14	+ 2O	18.6	646	497, 396, 628, 545, 453, 527, 277
M15	+ 2O	25.2	646	497, 628, 379, 396, 293, 388
M16	+ 2O	26.3	646	481, 628, 380, 363, 293, 372
M17	− 3-methylpyridine + O	22.9	539	390, 372, 503, 438, 289, 420
M18	− 3-methylpyridine + O	25.8	539	374, 356, 503, 273, 438, 420
substrate	indinavir	27.4	614	513, 495, 465, 421, 364, 277

[a] Retention time of the metabolites (min)

third scan event resulted in the selection m/z 364 for IND and its fragmentation to ions at m/z 272 and 174, which could be used to pinpoint the positional changes on the piperazine and pyridine portion of the molecule (Figure 2B).

Elemental Composition Confirmation of the Assigned Indinavir Fragment Ions. Although the interpretation of tandem mass spectrometry of IND was straightforward for most product ions (Figure 2), the m/z 421 could be assigned to two different structures (Supporting Information Figure 1); one appeared to be a radical cation according to the nitrogen rules.[22] Interestingly, the m/z 421 was the major product ion of IND using either Q-TOF (Supporting Information, Figure 2) or triple quadrupole mass spectrometers;[8,21] however, this ion was not detectable by the classical ion trap instruments with no wideband activation feature.[10] Since the interpretation of the substrate fragment ions is crucial for the proper assignment of the metabolites' structure, we obtained complementary elemental composition data on IND (Table 2), similar to the earlier proposed metabolite profiling strategy.[5]

The elemental composition assignments for major product ions of IND (Table 2), based on the accurate mass measurements, were consistent with the interpretation of IND product ions obtained by ion trap (Figure 2). The accurate mass of m/z 421.2367 revealed the molecular formula of $C_{25}H_{31}N_3O_3$ (0.3 ppm error) as structure A (Supporting Information, Figure 1), which is consistent with the earlier structural assignment.[8,21] This revealed the radical cation nature of m/z 421, consistent with the nitrogen rule for odd-electron ions with an odd number of nitrogen atoms.[22]

Knowledge-Based Metabolic Prediction for Indinavir. The list-dependent data acquisition strategy requires prior knowledge of metabolites' masses in order to preferentially trigger the MS^n fragmentation against the highly intense matrix signals. This, in turn, necessitates prerequisite information on the metabolites' structure and m/z. The comprehensive database of metabolism information, such as MDL Metabolite or Accelrys' Metabolism has become available in recent years. Therefore, the metabolic pathways of a given substrate could be predicted on the basis of the knowledge-based information available for similar structures. We outlined the potential metabolic pathways of IND in advance and further confirmed this scheme (Figure 3) by conducting a substructural similarity search on the MDL Metabolism Database. The substructure similarity search of 60% for IND using the MDL metabolite browser resulted in 188 hits. The MDL metabolite browser highlighted all theoretically expected metabolites on the basis of the number of functional groups found in the IND molecule, which included two hydrolytic, two N-dealkylated, three *N*-glucuronide, one N-methylated, and a few aliphatic and aromatic monooxygenated pathways.

Calculation of Mass-to-Charge Ratios for Indinavir Metabolites. The mass-to-charge ratios for IND metabolites were calculated using an active spreadsheet that incorporated common biotransformation[15,16] mass changes (Table 3). This spreadsheet also includes the mass change of common multistep metabolic reactions that authors encountered on various substrates. The mass-to-charge ratios utilized to set up the list-dependent data-acquisition method for IND were for the primary oxidative and dealkylated metabolic pathways, often responsible for the poor metabolic stability of NCEs.[3,23] In addition, the rare and multistep reactions such as the *N*-glucuronide metabolites for the parent (m/z 790) and its dealkylated product (m/z 699), as well as the acyl glucuronide of the carboxylic acid (m/z 483) dealkylated moiety (m/z 659), was included.

This table could also be used retrospectively to find the potential reactions responsible for certain unexpected metabolites' masses found in the full scan spectrum.[5] Since the parallel data acquisition strategy also requires the m/z of potential metabolites before setting multiple MS/MS experiments,[5] the complete list of biotransformation mass changes is presented in Table 3 for scientists who wish to use either approach.

(21) Gangl, E.; Utkin, I.; Gerber, N.; Vouros, P. *J. Chromatogr., A* **2002**, *974*, 91−101.

(22) McLafferty, F. W.; Turecek, F. *Interpretation of mass spectra*, 4th ed.; University Science Books: Sausalito, CA, 1993.

(23) Rodrigues, A. D. *Pharm. Res.* **1997**, *14*, 1504−1510.

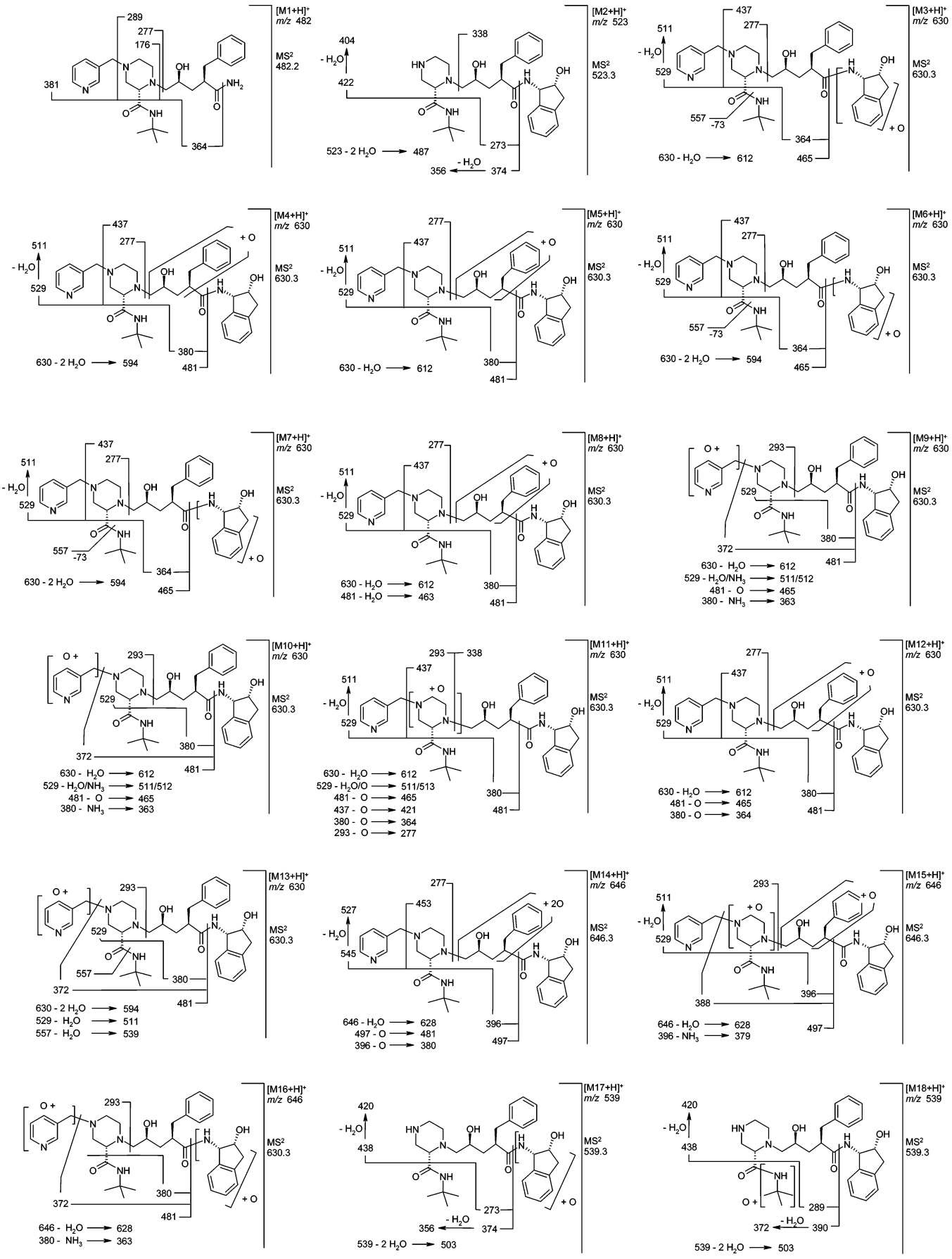

Figure 6. Proposed structures of 18 metabolites of indinavir from human hepatic S9 preparations.

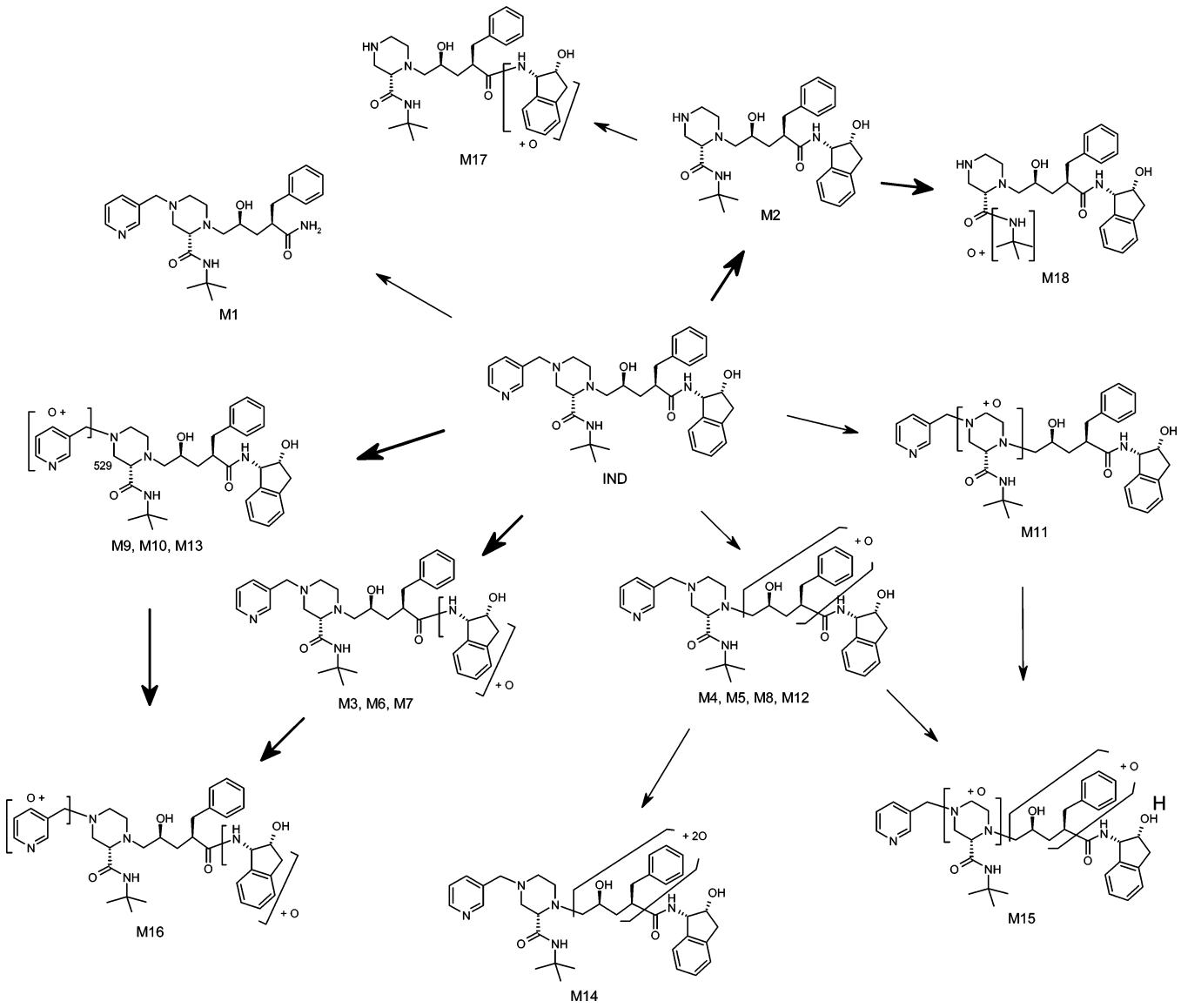

Figure 7. Proposed pathway of indinavir metabolism by human hepatic S9 preparations.

List-Dependent LC/MS^n Method for Metabolic Profiling of Indinavir. Although the full data-dependent qualitative analysis is appealing in theory, its practical value for biological mass spectrometry is hindered because of an overwhelming matrix signal. The components of biological matrixes are generally ionized and detected well under electrospray ionization,[24−27] which is preferentially used for metabolite identification because of its soft ionization nature.[7,28] As shown in Figure 4, the full data-dependent analysis of the extracts from incubation of IND with human hepatic S9 fractions resulted mainly in selection of highly intense biological matrix signals and unmetabolized IND for MS^n analysis. On the other hand, the list-specific data-dependent (list-dependent) analysis for ions m/z 603 and 523 resulted in the successful triggering of MS^n acquisition for the corresponding hydroxylated and dealkylated IND metabolites, even though the signal intensities of the metabolites were an order of magnitude less than that of the background matrix. Therefore, the list-dependent data acquisition is utilized in our approach, instead of full data-dependent MS^n function, to maximize the useful tandem mass spectral information obtained on the metabolites' structures (Figure 1).

Metabolism of Indinavir by Human Hepatic Postmitochondrial Preparation. This list-dependent instrument method, which included the wideband activation feature (Table 1), was used to look at the metabolites of IND generated by a human hepatic S9 preparation. The reconstructed ion chromatograms of all metabolites detected from the incubation of IND (10 μM) with human hepatic S9 are shown in Figure 5. Two dealkylated (M1, M2), 11 monooxygenated (M3-M13), 3 dioxygenated (M14-M16), and 2 dealkylated/monooxygenated (M17, M18) metabolites were detected with only a single LC/MS^n run (Figure 5). The m/z and major product ions of each metabolite are summarized in Table

(24) Enke, C. G. *Anal. Chem.* **1997**, *69*, 4885−4893.
(25) Cech, N. B.; Enke, C. G. *Mass Spectrom. Rev.* **2001**, *20*, 362−387.
(26) Matuszewski, B. K.; Constanzer, M. L.; Chavez-Eng, C. M. *Anal. Chem.* **1998**, *70*, 882−889.
(27) King, R.; Bonfiglio, R.; Fernandez-Metzler, C.; Miller-Stein, C.; Olah, T. *J. Am. Soc. Mass Spectrom.* **2000**, *11*, 942−950.
(28) Baillie, T. A.; Pearson, P. G.; Rashed, M. S.; Howald, W. N. *J. Pharm. Biomed. Anal.* **1989**, *7*, 1351−1360.

4. Using the assigned structural fragments for IND (Figure 2), supported by the elemental composition data (Table 2), the tentative structure of each metabolite was identified, as shown in Figure 6. On the basis of the intensity of each metabolite's reconstructed ion chromatogram, assuming similar ionization for the parent drug and its metabolites due to minor structural changes, three major metabolic pathways were shown to be responsible for biotransformation of IND by human liver S9 fraction (Figure 7). This is consistent with earlier in vitro metabolic profiling studies using human hepatic preparations, [^{14}C]-indinavir radiotracer, NMR, and synthetic standards,[18,20,29] indicating oxidation of pyridine (M9, M10), indanyl (M3), and phenylmethyl (M4, M5) moieties as well as N-dealkylation at piperazinyl (M2) as the major metabolic soft spots.

CONCLUSIONS

An early assessment of the metabolic fate of NCEs in preclinical research relies mainly on the information obtained from mass spectral analysis of biological samples. The present study describes the metabolic profiling of indinavir throughout an approach that integrates prerequisite knowledge-based predictions with the liquid chromatography data-dependent multistage tandem mass spectrometry. The knowledge-based metabolic prediction and metabolites' m/z calculation were carried on parallel to the study of the substrate fragmentation pattern before setting up a list-dependent LC/MS^n instrument method. Using human hepatic S9 preparations, 2 dealkylated, 11 monooxygenated, 3 dioxygenated, and 2 dealkylated/monooxygenated metabolites were detected using a single LC/MS^n analysis. The major metabolic pathways identified for in vitro metabolism of indinavir were identical to those found in earlier studies, demonstrating the capability of this integrated metabolite identification strategy in preclinical research to rapidly identify major metabolic pathways of a given drug.

(29) Lin, J. H. *Ernst Schering Res. Found Workshop* **2002**, 33−47.

ACKNOWLEDGMENT

We are grateful to Drs. David C. Evans and Paul G. Pearson, Department of Drug Metabolism, Merck Research Laboratories, for their suggestions and helpful discussions.

SUPPORTING INFORMATION AVAILABLE

Proposed structures for the indinavir product ion m/z 421 and the product ion spectrum of the protonated indinavir using Q-TOF mass spectrometry. This material is available free of charge via the Internet at http://pubs.acs.org.

Received for review August 21, 2003. Accepted November 12, 2003.

AC034980S